

In-situ growth of metal nanoparticles on boron nitride nanosheets as highly efficient catalysts

Li Fu^{a,b}, Guoxin Chen^b, Nan Jiang^b, Jinhong Yu^b, Cheng-Te Lin^{b,*} and Aimin Yu^{a,*}

^a Department of Chemistry and Biotechnology, Faculty of Science, Engineering and Technology, Swinburne University of Technology, Hawthorn VIC, Australia

E-mail: aiminyu@swin.edu.au

^b Key Laboratory of Marine New Materials and Related Technology, Zhejiang Key Laboratory of Marine Materials and Protection Technology, Ningbo Institute of Material Technology and Engineering, Chinese Academy of Sciences, Ningbo 315201, PR China

E-mail: linzhengde@nimte.ac.cn

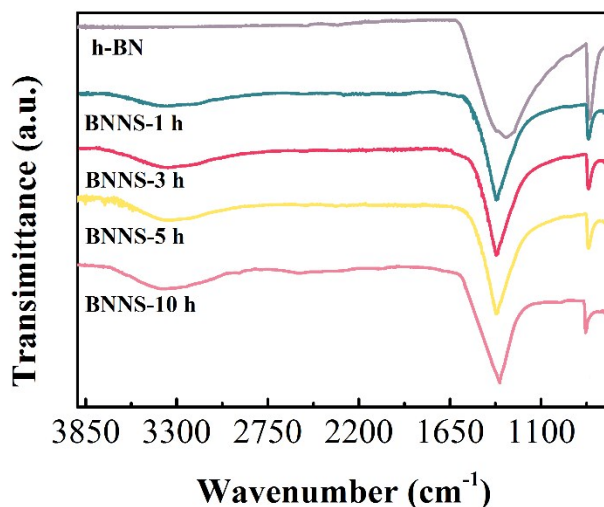


Fig. S1 FTIR spectra of pristine h-BN powder and BNNS collected after 1 h, 3h, 5h and 10h tip-sonication.

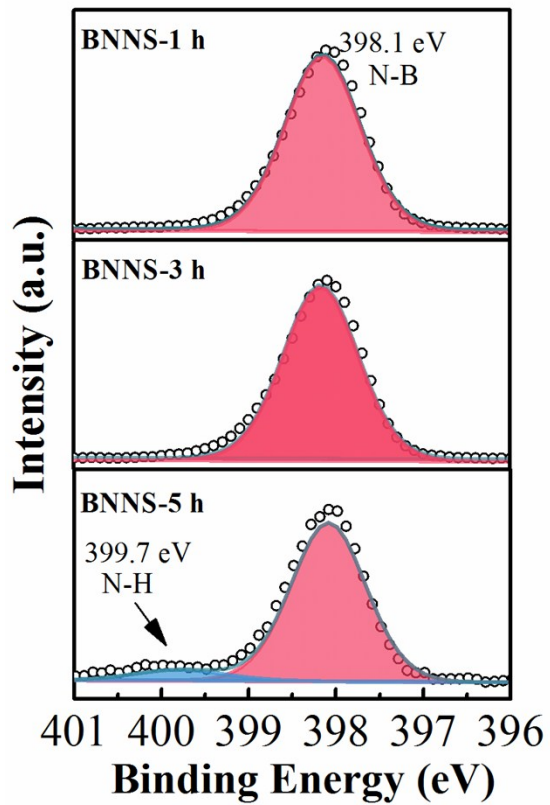


Fig. S2 N 1s narrow XPS scans of BNNS exfoliated in NaOH-water system for 1 h, 3 h and 5 h.

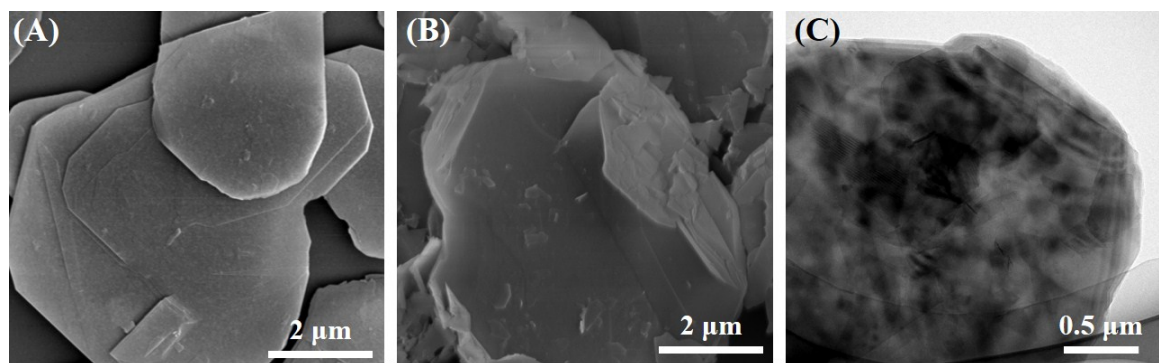


Fig. S3 SEM images of (A) pristine h-BN and (B) h-BN residue after exfoliation. (C) TEM image of pristine h-BN.

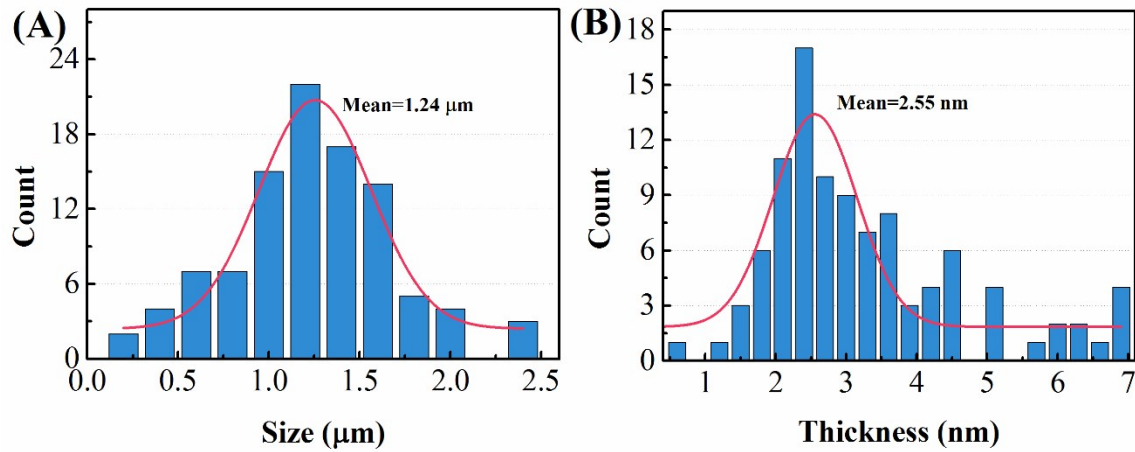


Fig. S4 (A) Lateral size distribution and (B) thickness distribution of BNNS.

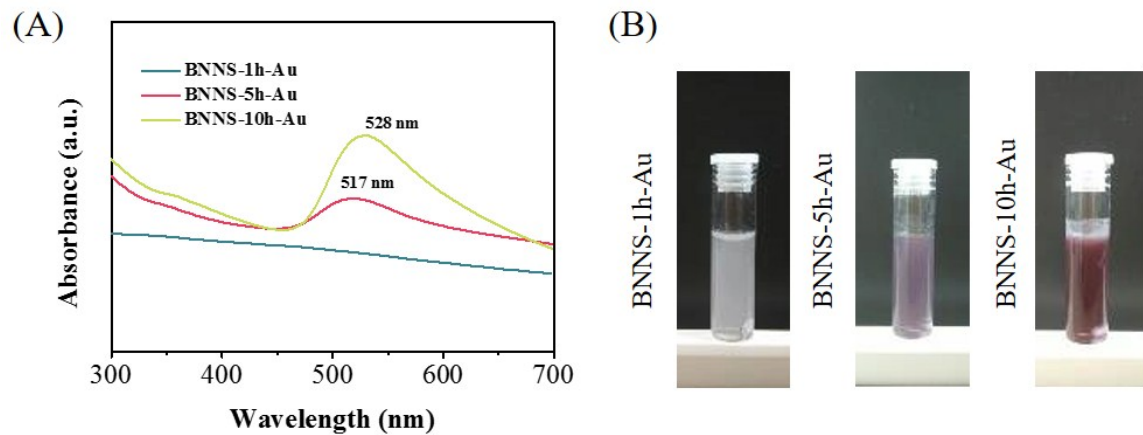


Fig. S5 (A) UV-vis spectra of BNNS, BNNS-5h-Au and BNNS-10h-Au nanocomposites. (B) Digital photos of BNNS-1h-Au, BNNS-5h-Au and BNNS-10h-Au.

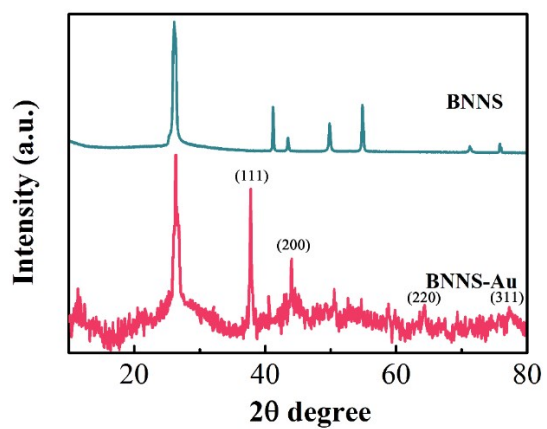


Fig. S6 XRD patterns of BNNS and BNNS-Au nanocomposite.

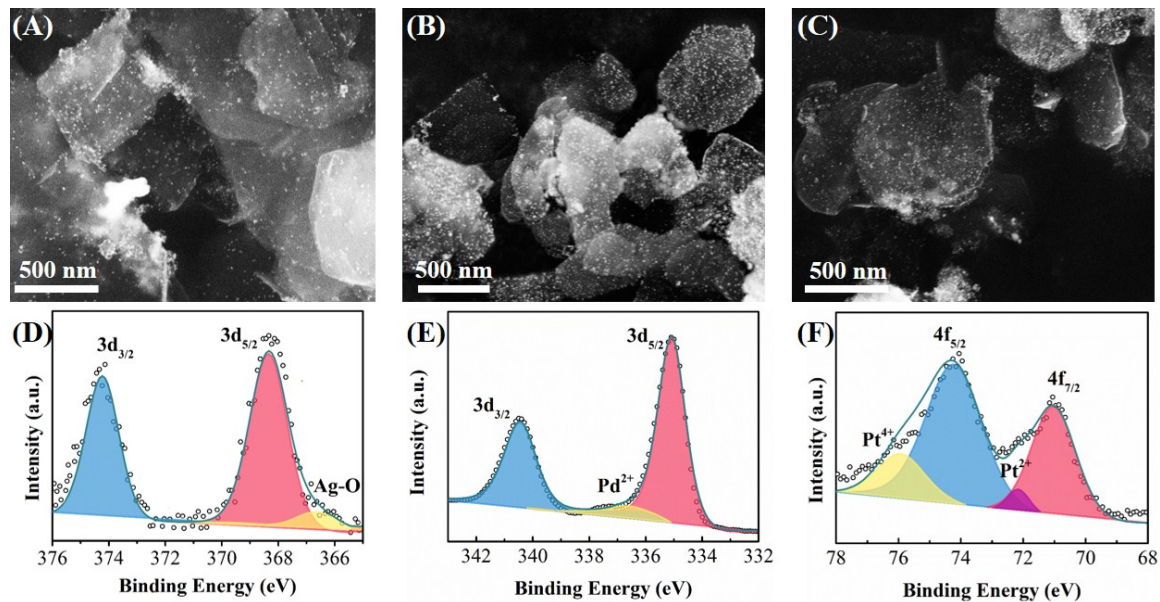


Fig. S7 SEM images of (A) BNNS-Ag, (B) BNNS-Pd and (C) BNNS-Pt nanocomposites. (D) Ag 3d narrow XPS scan of BNNS-Ag nanocomposite. (E) Pd 3d narrow XPS scan of BNNS-Pd nanocomposite. (F) Pt 4f narrow XPS scan of BNNS-Pt nanocomposite.

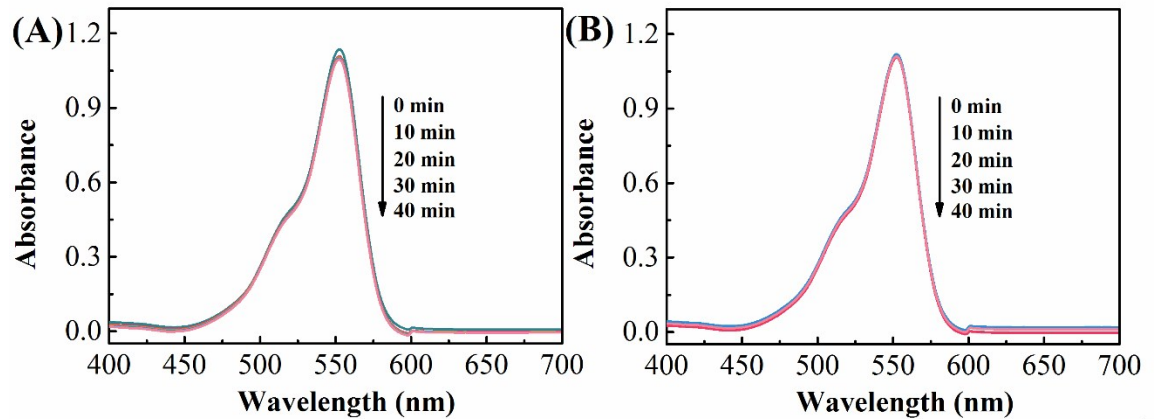


Fig. S8 UV-visible spectra of Rh B during the reduction process in the presence of (A) NaBH_4 and (B) BNNS+ NaBH_4 .

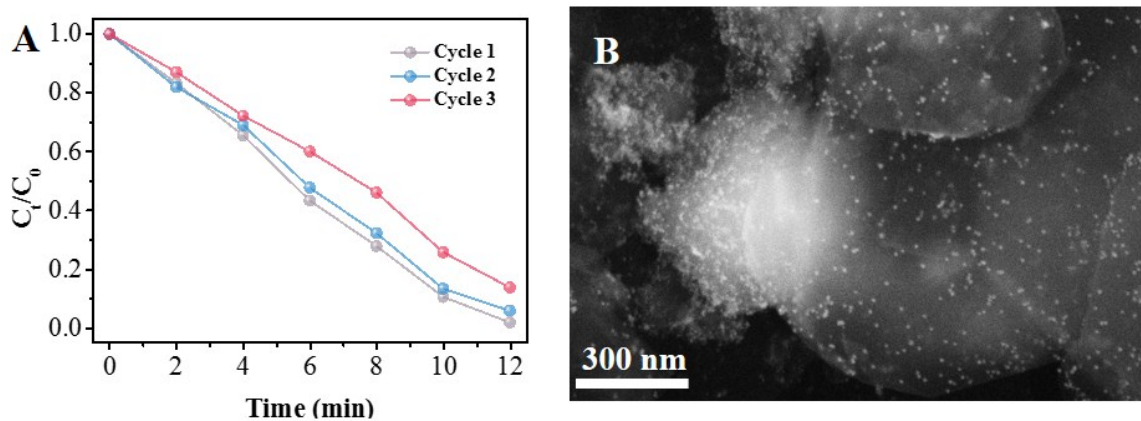


Fig. S9 (A) The catalytic performance of BNNS-Au NP composite for 3 cycles Rh B degradation. (B) SEM image of BNNS-Au NP composite after 3 cycles Rh B degradation.

Table S1 Performance comparison of the proposed BNNS-Au nanocomposite and other reported catalysts towards the reduction of RhB.

Catalyst	Rate constant (min ⁻¹)	Reference
Bimetallic Pt–Cu	2.7	1
Ag-Fe ₃ O ₄	0.42	2
Polydopamine microparticles	0.328	3
Sm-doped CeO ₂	0.161	4
BNNS-Au	0.064	This work

Table S2 Performance comparison of the proposed BNNS/Au/GCE and other electrodes towards the electrochemical detection of hydrazine.

Electrode	Method	LOD (μM)	Linear range (μM)	Reference
CeO ₂ -OMC*/GCE	I-T	0.012	0.04-192	5
Au@Pd-TiO ₂ NTs*/GCE	I-T	0.012	0.06-700	6
Au@Pd-rGO*/GCE	I-T	0.08	2-40	7
rGO-ZnO/GCE	I-T	0.8	1-33500	8
DHsalophen isomers/GCE	CV	1.6	10-400; 400-4000	9
Polypyrrole NWs*- AuNPs/GCE	DPV	0.2	1-500; 500-7500	10
BNNS-Au/GCE	DPV	0.0014	0.0005-0.5; 0.5-20; 20-2500	This work

*OMC = ordered mesoporous carbon *NTs = nanotubes *rGO = reduced graphene oxide *NWs = nanowires

References

1. H. P. Singh, N. Gupta, S. K. Sharma and R. K. Sharma, *Colloids and Surfaces A: Physicochemical and Engineering Aspects*, 2013, **416**, 43-50.
2. L. Ai, C. Zeng and Q. Wang, *Catalysis Communications*, 2011, **14**, 68-73.
3. S. Du, Z. Liao, Z. Qin, F. Zuo and X. Li, *Catalysis Communications*, 2015, **72**, 86-90.
4. S. Kundu, N. Sutradhar, R. Thangamuthu, B. Subramanian, A. B. Panda and M. Jayachandran, *Journal of Nanoparticle Research*, 2012, **14**, 1-16.
5. Y. Liu, Y. Li and X. He, *Anal. Chim. Acta.*, 2014, **819**, 26-33.
6. X. Chen, W. Liu, L. Tang, J. Wang, H. Pan and M. Du, *Materials Science and Engineering: C*, 2014, **34**, 304-310.

7. S. Dutta, C. Ray, S. Mallick, S. Sarkar, A. Roy and T. Pal, *RSC Advances*, 2015, **5**, 51690-51700.
8. J. Ding, S. Zhu, T. Zhu, W. Sun, Q. Li, G. Wei and Z. Su, *RSC Advances*, 2015, **5**, 22935-22942.
9. M. Revenga-Parra, E. Lorenzo and F. Pariente, *Sensors and Actuators B: Chemical*, 2005, **107**, 678-687.
10. J. Li and X. Lin, *Sensors and Actuators B: Chemical*, 2007, **126**, 527-535.